Severe liver degeneration and lack of *NF-κB* activation in *NEMO/IKKγ*-deficient mice

Dorothea Rudolph,[1] Wen-Chen Yeh,[1] Andrew Wakeham,[1] Bettina Rudolph,[2] Dhani Nallainathan,[1] Julia Potter,[1] Andrew J. Elia,[1] and Tak W. Mak[1,3]

[1]The Amgen Institute, Ontario Cancer Institute, and Departments of Medical Biophysics and Immunology, University of Toronto, Toronto, Ontario M5G 2C1, Canada; [2]Imperial Cancer Research Fund, WC2A 3PX London, UK

Phosphorylation of IκB, an inhibitor of *NF-κB*, is an important step in the activation of the transcription factor *NF-κB*. Phosphorylation is mediated by the IκB kinase (IKK) complex, known to contain two catalytic subunits: *IKKα* and *IKKβ*. A novel, noncatalytic component of this kinase complex called *NEMO* (*NF-κB* essential modulator)/*IKKγ* was identified recently. We have generated *NEMO/IKKγ*-deficient mice by gene targeting. Mutant embryos die at E12.5–E13.0 from severe liver damage due to apoptosis. *NEMO/IKKγ*-deficient primary murine embryonic fibroblasts (MEFs) lack detectable *NF-κB* DNA-binding activity in response to TNFα, IL-1, LPS, and Poly(IC) and do not show stimulus-dependent IκB kinase activity, which correlates with a lack of phosphorylation and degradation of IκBα. Consistent with these data, mutant MEFs show increased sensitivity to TNFα-induced apoptosis. Our data provide in vivo evidence that *NEMO/IKKγ* is the first essential, noncatalytic component of the IKK complex.

[*Key Words*: *NEMO/IKKγ*; *IKK*; *NF-κB*; liver apoptosis]

Received November 16, 1999; revised version accepted February 23, 2000.

The transcription factors of the *Rel/NF-κB* family are critical regulators of genes involved in inflammatory, immune and acute phase responses, proliferation, and apoptosis (Baeuerle and Henkel 1994). *NF-κB* activation is tightly controlled by IκB proteins. In resting cells, *NF-κB* is bound by IκB proteins, which mask the nuclear localization signal of *NF-κB* and prevent its nuclear translocation. Stimulation of the cell by a variety of stimuli, including proinflammatory cytokines such as tumor necrosis factor (TNFα) and interleukin-1 (IL-1), bacterial lipopolysaccharide (LPS) or viral infection, leads to the phosphorylation of IκB proteins on two conserved serine residues (Ser-32 and Ser-36 on IκBα and Ser-19 and Ser-23 on IκBβ) (DiDonato et al. 1996). The phosphorylated IκB proteins become targets for ubiquitination and proteasome-mediated degradation, consequently releasing *NF-κB* and allowing its translocation into the nucleus (Verma et al. 1995).

Recently, an IκB kinase activity was identified as a large complex, which contains two catalytic subunits, *IKKα* and *IKKβ* (DiDonato et al. 1997; Mercurio et al. 1997; Regnier et al. 1997; Woronicz et al. 1997; Zandi et al. 1997). These kinases are 52% identical and share several structural domains, including an amino-terminal kinase domain, a helix–loop–helix (HLH) domain and a leucine zipper (LZ) domain (Mercurio et al. 1997; Zandi et al. 1997). *IKKα* and *IKKα* form homo- and heterodimers in vitro, although only heterodimers are found in vivo (Woronicz et al. 1997). In vitro phosphorylation assays have shown that both kinases can phosphorylate IκBα on Ser-32 and Ser-36, but *IKKβ* seems to be more active in this regard (Woronicz et al. 1997). In addition, whereas *IKKβ* phosphorylates both critical serine residues of IκBα and IκBβ with equal efficiency (Woronicz et al. 1997), *IKKα* preferentially phosphorylates IκBβ on Ser-23 (Regnier et al. 1997). Catalytically inactive forms of both kinases inhibited TNFα and IL-1-induced *NF-κB* activation (Mercurio et al. 1997; Regnier et al. 1997; Woronicz et al. 1997; Zandi et al. 1997), suggesting that the kinases would have similar physiological functions. Surprisingly, recent gene targeting experiments have shown that, even though *IKKα* and *IKKβ* are part of the same IKK complex, share sequence homology and seem to have similar activities in vitro, *IKKα*-deficient mice and *IKKβ*-deficient mice have completely different phenotypes and the kinases seem to respond to different biological inducers. Although *IKKβ* mediates the response to proinflammatory cytokines such as TNFα and IL-1 (Li et al. 1999b; Z. Li et al. 1999; Tanaka et al. 1999), *IKKα* seems to respond to an unknown morphogenetic signal (Hu et al. 1999; Li et al. 1999a; Takeda et al. 1999). *IKKβ*$^{-/-}$ mice die at E12.5 to E14.5 from liver degeneration due to apoptosis (Li et al. 1999b; Z. Li et al. 1999;

[3]Corresponding author.
E-MAIL t.mak@oci.utoronto.ca; FAX (416) 204-2278.

Tanaka et al. 1999), a phenotype similar to, but more severe than, that of *RelA*$^{-/-}$ mice (Beg et al. 1995). In contrast, *IKKα*$^{-/-}$ mice survive to term but die shortly after birth (Hu et al. 1999; Li et al. 1999a; Takeda et al. 1999). *IKKα*$^{-/-}$ mice display rudimentary limbs and a tail as well as severe craniofacial deformities and skeletal abnormalities. Lack of *IKKα* also affects skin development, because the mutant epidermis shows increased thickness due to hyperproliferation of cells at the basal layer and a block in keratinocyte differentiation.

Two additional subunits of the IκB kinase complex have now been identified, *IKAP* (IKK-complex-associated protein) (Cohen et al. 1998), a potential scaffold protein, and *NEMO* (*NF-κB* essential modulator) (Yamaoka et al. 1998), also called *IKKγ* (Rothwarf et al. 1998) or *IKKAP1* (IκB kinase-associated protein 1) (Mercurio et al. 1999). *NEMO/IKKγ* is a glutamine-rich protein of 48 kD, which lacks a catalytic domain but contains two coiled–coil motifs and a LZ. *NEMO/IKKγ* seems to be essential for *NF-κB* activation. Introduction of a cDNA encoding *NEMO/IKKγ* was able to restore *NF-κB* DNA-binding activity in two cell lines with defective *NF-κB* activation (Yamaoka et al. 1998). Considering that both catalytic subunits of the IKK complex, *IKKα* and *IKKβ*, show similar in vitro activities but turned out to have very different physiological functions in vivo, we have generated *NEMO/IKKγ*-deficient mice to analyze the physiological relevance of this noncatalytic subunit of the IKK complex. In particular, we were curious to find out whether the phenotype of *NEMO/IKKγ*-deficient mice would be similar to the phenotype observed in *IKKα*- or *IKKβ*-deficient mice.

NEMO/IKKγ-deficient mice die at E12.5–E13.0 from severe liver degeneration due to apoptosis. *NEMO/IKKγ*-deficient primary murine embryonic fibroblasts (MEFs) show no detectable *NF-κB* DNA-binding activity in response to stimulation with TNFα, IL-1, LPS, or Poly(IC). Stimulus-dependent phosphorylation and degradation of IκBα is absent in mutant MEFs and IκB kinase activity is not detectable. Mutant MEFs are highly sensitive to TNFα and display reduced viability in response to TNFα treatment even in the absence of cycloheximide.

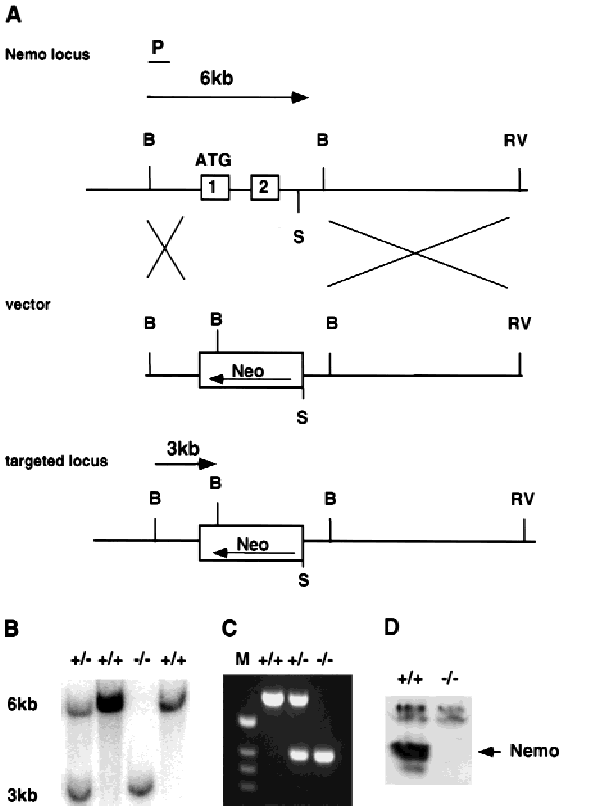

Figure 1. Generation of *NEMO/IKKγ*$^{-/-}$ mice. (*A*) Wild-type *NEMO/IKKγ* locus (*top*). Exon 1 and 2 are shown as open boxes and the ATG translation start site is indicated. (P) External flanking probe, (B) *Bam*HI, (RV) *Eco*RV, (S) *Spe*I. The targeting vector (*middle*) was designed to replace exon 1 and exon 2 of the wild-type locus with a neomycin cassette in antisense orientation. Flanking probe P detects a 6-kb *Bam*HI fragment corresponding to the wild-type allele and a 3-kb *Bam*HI fragment for the targeted allele (*bottom*). (*B*) Genomic Southern blot of *Bam*HI-digested DNA from E12.5 embryos of the indicated genotypes, showing the 6-kb wild-type band and the 3-kb mutant band detected by probe P. (*C*) Genotyping by PCR of DNA from E12.5 embryos using the primers described in Material and Methods. (*D*) Western blot analysis of *NEMO/IKKγ* protein expression in cytoplasmic extracts of MEFs of the indicated genotypes.

Results

Generation of NEMO/IKKγ*-deficient mice*

A targeting vector was designed to replace exon 1, encoding the translation start site, and exon 2 with a PGK–neo cassette (Fig. 1A). Correctly targeted ES cell clones were identified by Southern blot analysis and three ES clones were injected into C57BL/6 blastocysts to generate chimeric mice. Chimeric mice from all three clones transmitted the targeted *NEMO/IKKγ*-allele to their progeny. Genotypes were confirmed by Southern blot (Fig. 1B) and PCR analysis (Fig. 1C). *NEMO/IKKγ* has been mapped to the X chromosome (Jin and Jeang 1999; data not shown). Therefore, we could only generate heterozygous females from intercrosses of chimeric males with C57BL/6 females, which were then mated with C57BL/6 males to generate homozygous mutant mice. Although *NEMO/IKKγ*$^{+/-}$ females appeared normal and were fertile, viable homozygous mutant mice could not be generated from matings with C57BL/6 males, suggesting that a lack of *NEMO/IKKγ* results in embryonic lethality.

Western blot analysis of protein extracts from *NEMO/IKKγ*-deficient MEFs confirmed the absence of *NEMO/IKKγ* protein in mutant cells (Fig. 1D), indicating that we have generated a *NEMO/IKKγ* null mutation. We also did not detect changes in protein levels of *IKKα*, *IKKβ*, IκBα, or p65 (*RelA*) in mutant cells (data not shown).

Liver degeneration in NEMO/IKKγ*-deficient embryos*

Extensive timed matings were performed (Table 1).

Table 1. *Genotypes of embryos derived from matings of* NEMO/IKKγ$^{+/-}$ *females with C57BL/6 males*

Stage	+/+	+/−	−/−[a]	Total
E11.5	12	8	2	22
E12.5	54	29	20	103
E13.0	3	1	3	7
E13.5	13	5	2*	20
E14.5	6	2	1*	9

[a](*) In resorption.

NEMO/IKKγ$^{-/-}$ embryos were normal at E11.5. On sections of E12.5$^{-/-}$ embryos, areas of hemorrhaging and tissue loss were apparent in parts of the liver (Fig. 2A,B; data not shown). At E13.0–E13.5, mutant embryos were dead and anemic in appearance. Mutant embryos at these stages showed massive liver hemorrhages, which are most likely due to the breakdown of the liver architecture at this developmental stage (Fig. 2D). To determine whether the observed cell death in the liver was due to apoptosis, TUNEL assays were performed on sections of E11.5 and E12.5 wild-type and mutant embryos. Only a few isolated TUNEL-positive cells could be detected on sections from wild-type embryos at both stages (Fig. 2G; data not shown). Mutant embryos at E11.5 showed only a slightly increased number of TUNEL-positive cells in small areas of the liver (data not shown). However, by E12.5, greatly increased numbers of TUNEL-positive cells in large areas throughout the liver were observed in mutant embryos (Fig. 2H), suggesting that apoptosis in the liver is a major cause of death of the mutant embryos. Enhanced apoptosis in the mutant embryos appeared to be restricted to the liver, as other parts of the *NEMO/IKKγ*$^{-/-}$ embryos did not show an increase in TUNEL-positive cells. Cell proliferation in E12.5 mutant embryos as detected by BrdU incorporation was generally comparable with wild-type embryos (data not shown) except in the liver (Fig. 2E,F). Of note, sections of dorsal skin at E12.5, which at this stage consists of a single layer of cells with underlying mesenchyme, showed similar proliferation in wild-type and mutant skin (data not shown).

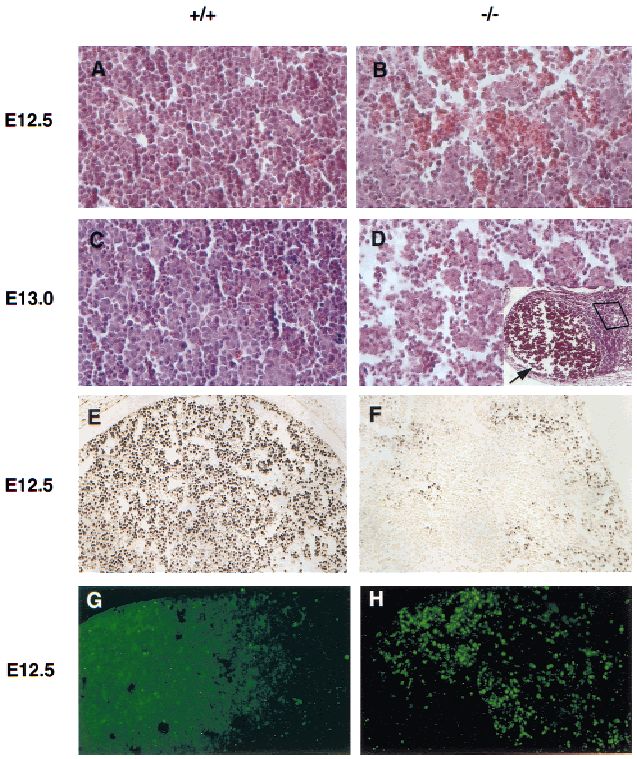

Figure 2. Massive liver apoptosis in the absence of *NEMO/IKKγ*. (*A–D*) Histological analysis of liver sections from E12.5 (*A,B*) and E13.0 (*C,D*) wild-type (*A,C*) and *NEMO/IKKγ*-deficient (*B,D*) embryos. Hematoxylin and eosin staining; high-power view. (*D*) The inset shows a low power view of the same region shown in *D*. The arrow points to a large area of tissue loss in which erythrocytes have accumulated. (*E,F*) Detection of cell proliferation as determined by BrdU incorporation. Pregnant females were injected IP with BrdU 60-min prior to sacrifice. Sections of E12.5 wild-type and mutant embryos were prepared and immunostained with anti-BrdU antibody. A high power view of the liver is shown. (*G,H*) Enhanced apoptosis in livers of E12.5 *NEMO/IKKγ*-deficient embryos. TUNEL assays were performed on sections of wild-type and mutant E12.5 embryos. A high power view of the liver is shown in both cases.

Lack of NF-κB *activation in* NEMO/IKKγ*-deficient MEFs*

The above-mentioned phenotype of *NEMO/IKKγ*$^{-/-}$ mice is similar to, albeit more severe than, that of *RelA*-deficient mice (Beg et al. 1995). *RelA* is a subunit of the most common form of *NF-κB*, the *p50–RelA* heterodimer. We therefore assessed whether the activation of *NF-κB* DNA-binding activity was impaired in *NEMO/IKKγ*-deficient MEFs. Wild-type and *NEMO/IKKγ*-deficient MEFs were treated with TNFα, IL-1, LPS, or poly(IC) to induce *NF-κB* DNA-binding activity and nuclear extracts were examined by gel shift assay. In contrast to wild-type MEFs, mutant MEFs showed no detectable *NF-κB* DNA-binding activity in response to any of these stimuli (Fig. 3; data not shown). Interestingly, *IKKα*$^{-/-}$ MEFs show normal *NF-κB* DNA-binding activity in response to these stimuli (Hu et al. 1999; Li et al. 1999a; Takeda et al. 1999), whereas *NF-κB* activation in *IKKβ*$^{-/-}$ MEFs is impaired, although it still occurred with delayed kinetics and reduced magnitude (Li et al. 1999b; Tanaka et al. 1999).

Lack of IκBα phosphorylation/degradation in NEMO/IKKγ*-deficient MEFs*

Next, we analyzed whether stimulus-dependent phosphorylation and degradation of IκBα was affected by the absence of *NEMO/IKKγ*. Wild-type and *NEMO/IKKγ*-deficient MEFs were stimulated with TNFα for 0, 6, and 10 min. Cytoplasmic extracts were prepared and used for Western blot analysis with an anti-phospho *IκBα*-specific antibody. Phosphorylation of *IκBα* could be de-

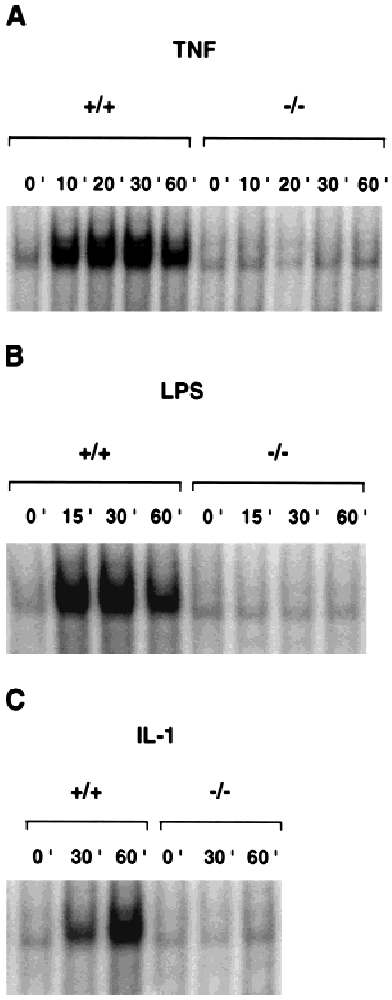

Figure 3. Impaired NF-κB activation in *NEMO/IKKγ*-deficient cells. Wild-type or *NEMO/IKKγ*$^{-/-}$ MEFs were incubated with mouse recombinant TNFα (10 ng/ml) (*A*), LPS (15 μg/ml) (*B*), or IL-1 (10 ng/ml) (*C*) for the indicated times. *NF-κB* activation in 10 μg of nuclear extract was determined by gel shift assay as described in Materials and Methods.

tected in wild-type cells as soon as 6 min after TNFα stimulation (Fig. 4A, top left). However, no phosphorylation of IκBα could be detected in extracts of *NEMO/IKKγ*-deficient MEFs even after 10 min stimulation with TNFα (Fig. 4A, top right). An anti-*IκBα* specific antibody was used as a control to detect IκBα protein expression in −/− extracts. (Fig. 4A, bottom). As shown in Figure 4B, IκBα is degraded in wild-type cells and reappears 30–60 min after stimulation (Fig. 4B, top), whereas degradation of IκBα is completely absent in mutant cells (Fig. 4B, bottom).

Impaired IκB kinase activity in NEMO/IKKγ*-deficient MEFs*

The failure to phosphorylate IκBα in the absence of *NEMO/IKKγ* prompted us to examine the in vitro kinase activity of the IKK complex. Wild-type and *NEMO/IKKγ*-deficient MEFs were treated for 7 min with TNFα

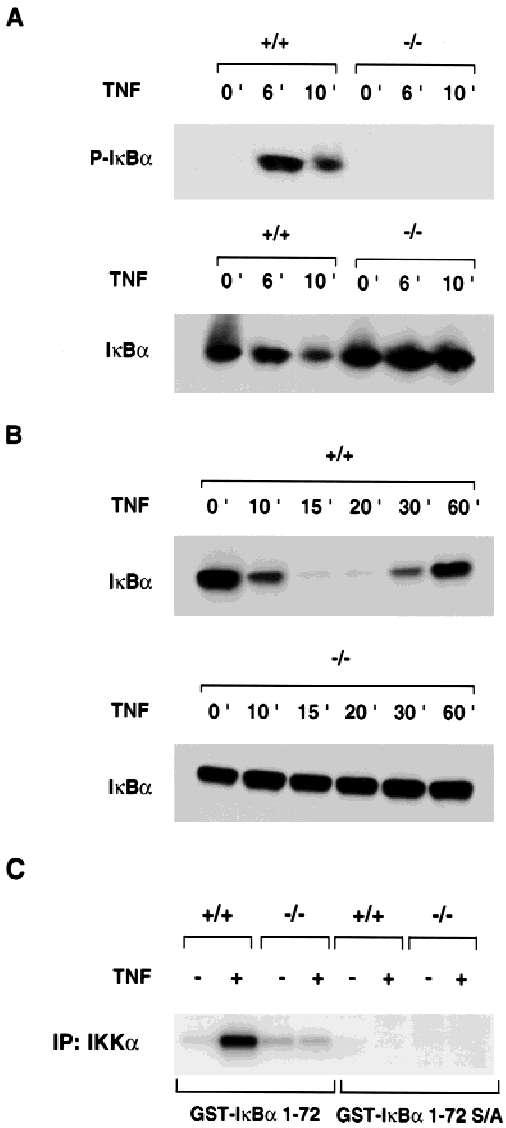

Figure 4. Defective TNFα-induced IκBα phosphorylation and degradation and IκB kinase activity in the absence of *NEMO/IKKγ*. (*A*) IκBα phosphorylation. (*Top*) Wild-type and *NEMO/IKKγ*-deficient MEFs were treated with TNFα (10 ng/ml) for the indicated times followed by Western blot analysis of cytoplasmic extracts with anti-phospho-*IκBα*-specific antibody. (*Bottom*) Western blot of the same extracts with anti-*IκBα* antibody as a control to show IκBα protein expression in mutant cells. (*B*) IκBα degradation. Wild-type (*top*) and *NEMO/IKKγ*-deficient (*bottom*) MEFs were treated with TNFα (10 ng/ml) for the indicated times followed by Western blot analysis with anti-*IκBα* specific antibody. (*C*) IκB kinase activity. Wild-type and *NEMO/IKKγ*-deficient MEFs were either left in medium alone or treated with TNFα (10 ng/ml) for 7 min. Whole cell extracts were immunoprecipitated with anti-*IKKα* antibody and in vitro kinase activity was determined as described in Materials and Methods using GST–IκBα (1–72) (*left*) or GST–IκBα (1–72) S/A (*right*) as a substrate. One representative experiment of four is shown.

to induce kinase activity. Whole cell extracts were immunoprecipitated with anti-*IKKα* antibody and kinase activity was assessed in vitro using GST–IκBα (1–72) or GST–IκBα (1–72) S/A, containing a Ser-32/Ser-36 to Ala-32/Ala-36 mutation as a substrate. Extracts of wild-type cells were able to phosphorylate GST–IκBα (1–72) in vitro, whereas stimulus-dependent kinase activity in extracts of *NEMO/IKKγ*-deficient MEFs was severely impaired (Fig. 4C), indicating that *NEMO/IKKγ* is essential for IκB kinase activity. Similar results were obtained with a longer substrate [GST–IκBα (1–317)] (data not shown).

Expression of NF-κB*-dependent target genes is impaired in* NEMO/IKKγ*-deficient MEFs*

The above data showed that *NF-κB* activation is defective in the absence of *NEMO/IKKγ*. We therefore examined the expression of known *NF-κB*-dependent target genes. *IκBα* is one of the first genes to be up-regulated following *NF-κB* activation, establishing a feedback loop, which will eventually shut down the *NF-κB* response. This induction, but not basal *IκBα* mRNA expression, is regulated by *RelA* (Scott et al. 1993). To analyze *IκBα* mRNA expression in the absence of *NEMO/IKKγ*, RNA from wild-type and *NEMO/IKKγ*-deficient MEFs treated with TNFα for 0, 30, and 60 min was analyzed by Northern blot. As shown in Figure 5A, an *IκBα* transcript induced within 60 min of TNFα stimulation in wild-type cells is absent in *NEMO/IKKγ*-deficient MEFs. Interestingly, *IKKβ*$^{-/-}$ MEFs are still able to express the TNFα-induced *IκBα* transcript, although the level of transcription is reduced compared with wild-type cells (Li et al. 1999b).

Stimulation of cells with IL-1 leads to expression of various genes, including interleukin-6 (IL-6), an important mediator of acute phase reactions. IL-1 induces IL-6 expression through the coordinated action of *NF-κB* and the transcription factor *NF-IL6* (Akira and Kishimoto 1992). We therefore treated wild-type and *NEMO/IKKγ*-deficient MEFs with IL-1 for 16 hr and measured the levels of IL-6 in the culture supernatant using an ELISA. Whereas wild-type MEFs showed stimulus-dependent production of IL-6, IL-1 treatment of mutant MEFs failed to up-regulate IL-6 expression (Fig. 5B). Levels of IL-6 in the stimulated *NEMO/IKKγ*-deficient cultures were equivalent to those in wild-type cultures treated with medium alone. These data demonstrate impaired induction of acute phase response proteins in the absence of *NEMO/IKKγ*.

Cells lacking *NF-κB* activity have been shown to undergo apoptosis in response to TNFα stimulation (Beg and Baltimore 1996; Van Antwerp et al. 1996; Wang et al. 1996), suggesting that *NF-κB* activation provides protection against TNFα-induced apoptosis. To determine whether sensitivity to TNFα-induced apoptosis was increased in the absence of *NEMO/IKKγ*, the viability of wild-type and *NEMO/IKKγ*-deficient MEFs after treatment with various concentrations of TNFα for 18 hr was assessed. Wild-type MEFs were resistant to TNFα-mediated cytotoxicity, but *NEMO/IKKγ* deficient MEFs showed a dramatic reduction in viability even in the absence of cycloheximide (Fig. 6A). TNFα-sensitivity of *NEMO/IKKγ*-deficient MEFs could be further increased by addition of very low concentrations of cycloheximide (30–100 ng/ml). Significantly higher concentrations of cycloheximide in combination with TNFα were required to affect viability of wild-type MEFs (Fig. 6B).

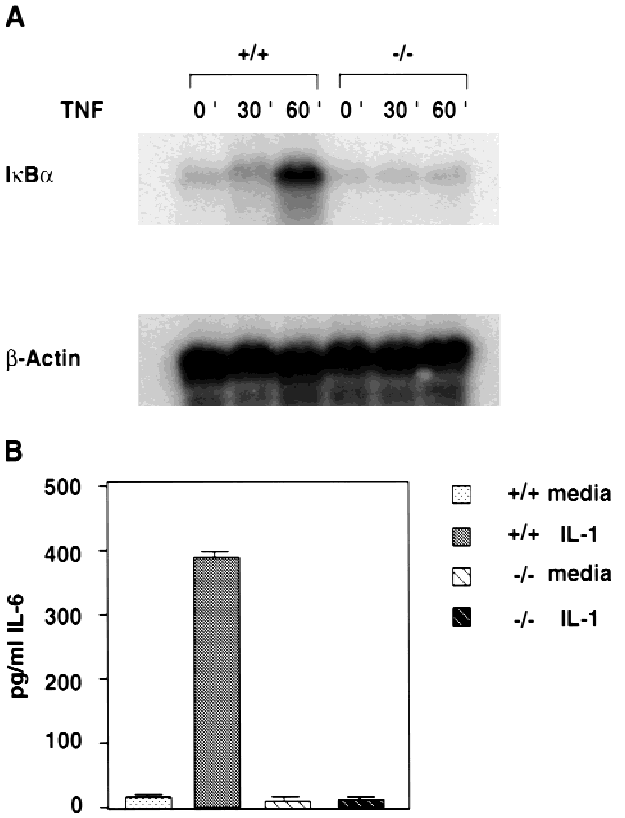

Figure 5. Impaired expression of *NF-κB* target genes in *NEMO/IKKγ*-deficient MEFs. (*A*) TNFα-induced *IκBα* mRNA synthesis. Wild-type and *NEMO/IKKγ*-deficient MEFs were stimulated with TNFα (10 ng/ml) for the indicated times and 20 μg of RNA was analyzed by Northern blot analysis using a ^{32}P-labeled random priming probe corresponding to the full-length *IκBα* cDNA. *β-actin*, loading control. (*B*) IL-1 induced IL-6 production. Wild-type and *NEMO/IKKγ*-deficient MEFs (3×10^4) were left untreated or stimulated with IL-1 (10 ng/ml) for 16 hr. Levels of IL-6 (pg/ml) in culture supernatants were determined by ELISA. Values shown are the mean and standard deviation of triplicate samples.

Discussion

In this study, we have shown that *NEMO/IKKγ*, a component of the IKK complex, is required for the phosphorylation and degradation of IκBα. Lack of *NEMO/IKKγ* affects IκB kinase activity, in particular also *IKKα* kinase activity (Fig. 4C). We have demonstrated that *NEMO/IKKγ* is crucial for normal stimulus-dependent *NF-κB* activation and target gene expression. *NEMO/*

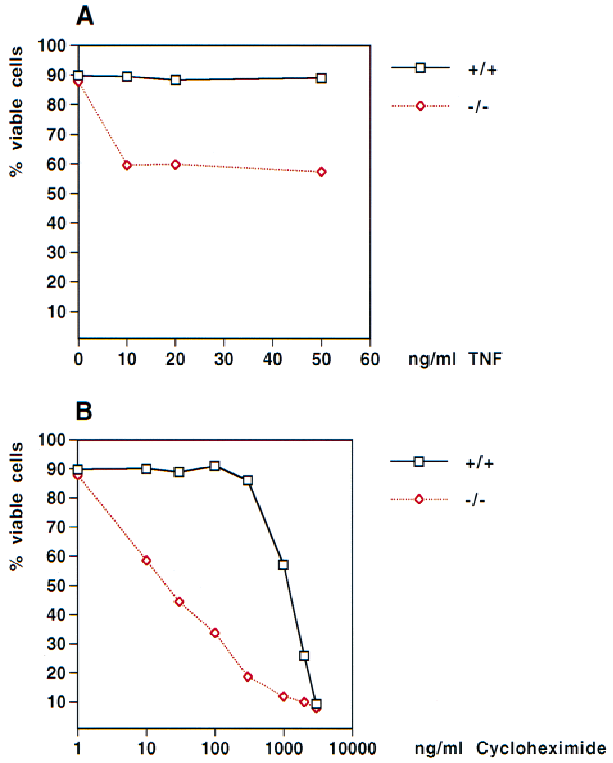

Figure 6. TNFα-induced cytotoxicity. (*A*) TNFα-induced cytotoxicity. Wild-type and *NEMO/IKK*γ-deficient (2×10^5) MEFs were left untreated or stimulated with the indicated concentrations of TNFα for 18 hr. Cells were then harvested and stained with PI/AnnexinV-FITC. Values shown are the percentage of viable cells after treatment relative to untreated controls. (*B*) Cytotoxicity induced by TNFα plus cycloheximide. Wild-type and *NEMO/IKK*γ-deficient MEFs (2×10^5) were left untreated or stimulated with TNFα (10 ng/ml) in combination with the indicated concentrations of cycloheximide for 18 hr. Cells were harvested and stained as described for *A*, and values shown were determined as for *A*.

*IKK*γ-deficient MEFs show increased sensitivity to TNFα treatment, implying that the liver apoptosis observed in *NEMO/IKK*γ-deficient mice could be due to a lack of *NF-κB*-mediated protection from TNFα cytotoxicity. *RelA*$^{-/-}$ and *IKKβ*$^{-/-}$ fibroblasts are also highly sensitized to TNFα in vitro (Beg et al. 1995; Li et al. 1999b; Tanaka et al. 1999). Interestingly, *RelA/TNFα* double-deficient mice (Doi et al. 1999) as well as *IKKβ/TNFR1* double-deficient mice (Li et al. 1999b) are born alive, consistent with the hypothesis that enhanced sensitivity to endogenous TNFα is responsible for the liver apoptosis observed in these mice.

*NEMO/IKK*γ is a noncatalytic component of the IκB kinase complex. Precisely how it functions within the complex remains to be clarified. Analysis of a *NEMO/IKK*γ-deletion mutant series showed that the carboxyl terminus of the protein (amino acids 300–419) is required for TNFα-stimulated IκB kinase activity but not basal kinase activity (Rothwarf et al. 1998). Furthermore, this mutation did not interfere with the binding of *NEMO/IKK*γ to *IKKα/β* in cells, suggesting that the carboxyl terminus might be required to connect the IKK complex to upstream activators. Gene-targeting experiments have shown that *IKKβ* rather than *IKKα* mediates the response to proinflammatory cytokines and that *IKKα* seems to respond to an unknown morphogenetic signal (Hu et al. 1999; Li et al. 1999a,b; Z. Li et al. 1999; Takeda et al. 1999; Tanaka et al. 1999). At E18.5, *IKKα*$^{-/-}$ mice display rudimentary limbs and a tail as well as severe craniofacial deformities and skeletal abnormalities. Takeda et al. (1999) and Li et al. (1999a) show that *IKKα*$^{-/-}$ embryos at E12.5 already have mild alterations in the morphology of the limb buds (Li et al. 1999a; Takeda et al. 1999), whereas Hu et al. (1999) state that at E14.5, the forelimbs and hindlimbs of *IKKα*$^{-/-}$ embryos are not significantly shorter than those of wild-type littermates. At E12.5, limbbuds of *NEMO/IKK*γ-deficient mice are indistinguishable from those of wild-type littermates (data not shown), even though kinase assays (Fig. 4C) showed that *IKKα* activity is severely impaired in extracts of *NEMO/IKK*γ-deficient MEFs. However, this does not exclude the possibility that *NEMO/IKK*γ-deficient mice would show a phenotype similar to that observed in *IKKα*-deficient mice at E18.5, if they survived until this developmental stage. Lack of *IKKα* also affects skin development because the mutant epidermis at E18.5 shows increased thickness due to hyperproliferation of cells at the basal layer and a block in keratinocyte differentiation (Hu et al. 1999; Li et al. 1999a; Takeda et al. 1999). However, at E12.5, proliferation of the skin as detected by BrdU incorporation is comparable in wild-type and *NEMO/IKK*γ-deficient embryos (data not shown). At E12.5, the skin consists of a single layer of cells with underlying mesenchyme. Epidermal differentiation does not occur until later in development. Therefore, we cannot exclude the possibility that *NEMO/IKK*γ-deficient mice would show defects in epidermal differentiation similar to those observed in *IKKα*-deficient mice at E18.5, if they survived until this developmental stage, especially as *IKKα* kinase activity is severely impaired in *NEMO/IKK*γ-deficient MEFs (Fig. 4C).

Overall, the phenotype observed in *NEMO/IKK*γ-deficient mice is more severe than that of *IKKβ*$^{-/-}$ mice. In particular, the onset of the liver phenotype occurs at least 12 hr earlier in *NEMO/IKK*γ-deficient embryos than in *IKKβ*$^{-/-}$ embryos. Even though *IKKβ*$^{-/-}$ embryos show hemorrhages in the liver on E13.0, the overall liver architecture is still intact (Li et al. 1999b). In contrast, *NEMO/IKK*γ-deficient embryos show large areas of tissue loss at this stage and a massive accumulation of erythrocytes. Moreover, *IKKβ*$^{-/-}$ MEFs still show residual *NF-κB* DNA-binding activity in response to stimulation with TNFα or IL-1 (Z. Li et al. 1999; Tanaka et al. 1999), whereas *NF-κB* DNA-binding activity in response to these stimuli is completely abolished in *NEMO/IKK*γ-deficient MEFs. This suggests that the residual *NF-κB* DNA-binding activity observed in *IKKβ*$^{-/-}$ mice might provide limited protection to liver cells against apoptosis induced by endogenous TNFα. The earlier onset of the phenotype in *NEMO/IKK*γ-deficient mice might then be explained by the complete absence

of *NF-κB* DNA-binding activity. As shown by Li et al. (1999b) the residual *NF-κB* DNA-binding activity observed in *IKKβ*$^{-/-}$ MEFs is still sufficient to induce a low level of expression of *NF-κB*-dependent target genes such as *IκBα* (Li et al. 1999b). Sixty minutes after TNFα stimulation of *IKKβ*$^{-/-}$ MEFs, about half the amount of *IκBα* mRNA observed in stimulated wild-type cells is detected in *IKKβ* mutant cells. However, *IκBα* mRNA is not induced at all in *NEMO/IKKγ*-deficient MEFs, which is consistent with the lack of detectable *NF-κB* DNA-binding activity in these cells.

In summary, the effects of the targeted disruption of the *NEMO/IKKγ* gene on *NF-κB* activation by a variety of stimuli are more dramatic than the deletion of either catalytic component of the IKK complex. We therefore speculate that the phenotype of *IKKα/IKKβ* double-deficient mice will be similar to that of *NEMO/IKKγ*-deficient mice. In any case, our data provide strong in vivo evidence that *NEMO/IKKγ* is essential for activation of *NF-κB* by various stimuli. Our study combined with previous reports clearly demonstrates that *NEMO/IKKγ* is the first essential, non-kinase component of the IKK complex.

Material and methods

Generation of NEMO/IKKγ*-deficient mice*

Phage clones containing the murine *NEMO/IKKγ* gene were isolated by screening a 129/J genomic library with a probe corresponding to the 5′ end of the NEMO cDNA (Yamaoka et al. 1998). A targeting vector was designed to replace exon 1 and exon 2 with a PGK–neo cassette in antisense orientation, leading to the replacement of the first 131 amino acids of the *NEMO/IKKγ* protein and a downstream frameshift. A total of 30 μg of the linearized targeting vector were used to electroporate 5×10^6 E14K ES cells (Bio-Rad Gene Pulser, 0.34 kV, 0.25 mF), which were subsequently cultured for 10 days in DMEM supplemented with 15% FBS, glutamine, pyruvate, β-mercaptoethanol, and leukemia inhibitory factor, containing 300 μg/ml G418 (Sigma). Recombinants were identified by PCR and confirmed by Southern blot analysis using *Bam*HI-digested genomic DNA hybridized to an external flanking probe, which detects a 6-kb band for the wild-type locus and a 3-kb band for the mutant allele. Single integration was confirmed using a probe corresponding to the *neo* gene. Three correctly targeted ES clones were injected into C57BL/6 blastocysts and all three successfully generated germ-line chimeras. Genotyping of mice was performed by PCR using tail genomic DNA with the following primers: 5′-ACTTAAAGGTGTGTGGAGGAGGTAG-G-3′, 5′-TGCATGTGACTCTTCACAGAGAACCC-3′, 5′-GG-GTGGGATTAGATAAATGCCTGCTC-3′. These primers give rise to a 621-bp PCR product for the wild-type locus and a 354-bp PCR product for the mutant allele. The following PCR conditions were used: 1 min at 95°C, 30 sec at 64°C, 1.5 min at 72°C, for 35 cycles.

Animal husbandry

Mice were maintained in the animal facility of the Ontario Cancer Institute in accordance with its ethical guidelines.

Histology

Embryos were fixed with 4% buffered formalin at 4°C for 12 hr and embedded in paraffin. Sections were stained with hematoxylin and eosin according to standard protocols. For the detection of BrdU incorporation, immunostaining with anti-BrdU antibody was performed on paraffin sections according to standard procedures. Pregnant females were injected with 300 μl of BrdU (10 mg/ml) 60 min prior to sacrifice. For determination of apoptosis, TUNEL assays were performed using an in situ cell death detection kit (Boehringer Mannheim) according to the manufacturer's instructions.

Generation of primary MEFs

Primary MEFs were derived from E12.5 embryos. The head and liver were removed and the remainder of the embryo was cut into small pieces and trypsinized. Cells were washed in medium and plated onto 6-well plates. Embryonic fibroblasts were expanded in DMEM supplemented with 10% FBS and β-mercaptoethanol and frozen.

Western blot analysis

Cytoplasmic extracts were prepared from primary MEFs as described previously (Yamaoka et al. 1998). Briefly, cells were stimulated, washed with cold PBS, resuspended at 10^6/20 μl in hypotonic solution [10 mM HEPES at pH 7.8, 10 mM KCl, 2 mM $MgCl_2$, 1 mM DTT, and 0.1 mM EDTA supplemented with a protease inhibitor cocktail (Boehringer Mannheim)] and kept on ice for 10 min. NP-40 was added to a final concentration of 1% and the cells were centrifuged at 14,000 rpm for 1 min. The supernatant, containing the cytoplasmic fraction, was recovered and the protein concentration was determined using a Bio-Rad protein assay. Protein samples were fractionated on a 10% SDS–polyacrylamide gel and blotted onto a PVDF membrane. Western blots were developed using an enhanced chemiluminescence system according to the manufacturer's instructions (Amersham). Anti-phospho-*IκBα* and anti-*IκBα* were from New England Biolabs. Anti-*NEMO* antiserum was kindly provided by Alain Israel (Institute Pasteur, Paris, France).

Gel mobility shift assay

MEFs (2×10^6) were lysed in 400 μl of hypotonic solution as described above and nuclear extracts were prepared for gel mobility shift assays as described previously (Yeh et al. 1997). A total of 10 μg of nuclear extract was incubated with an end-labeled, double-stranded oligo containing two *NF-κB* binding sites (5′-ATCAGGGACTTTCCGCTGGGGACTTTCCG-3′ and 5′-CGGAAAGTCCCCAGCGGAAAGTCCTGAT-3′). The reaction was performed in 20 μl of binding buffer (5 mM HEPES at pH 7.8, 50 mM KCl, 0.5 mM DTT, 1 μg of [poly d(I-C)], 10% glycerol] for 20 min at room temperature. Samples were fractionated on a 5% polyacrylamide gel and visualized by autoradiography.

Kinase assay

MEFs (5×10^6) were lysed as described previously (Tanaka et al. 1999). Briefly, cells were lysed with lysis buffer containing 50 mM HEPES (pH 7.6), 150 mM NaCl, 1.5 mM $MgCl_2$, 1 mM EGTA, 10% glycerol, 1% Triton X-100, protease inhibitor cocktail (Boehringer Mannheim), 20 mM β-glycerophosphate, 1 mM sodium orthovanadate, and 10 mM NaF. After incubation on ice for 30 min, lysates were centrifuged for 10 min at 14,000 rpm and the protein concentration of the supernatant was determined using the Bio-Rad protein assay. A total of 500 μg of protein extract was precleared using protein G–Sepharose (Phar-

macia) and immunoprecipitated with anti-*IKKα* (Santa Cruz). The immunoprecipitates were washed twice with lysis buffer and twice with kinase buffer [20 mM HEPES at pH 7.9, 10 mM $MgCl_2$, 100 mM NaCl, protease inhibitor cocktail (Boehringer Mannheim), 20 mM β-glycerophospate, 1 mM sodium orthovanadate, 2 mM DTT] and assayed for kinase activity as described previously (Tanaka et al. 1999) using [γ^{32}P]ATP and 3 μg of GST–IκBα (1–72) or GST–IκBα (1–72) S/A as a substrate. Reaction products were fractionated by 10% SDS-PAGE and phosphorylated IκBα was visualized by autoradiograhy.

Measurement of IL-6 production

MEFs (3×10^4) were plated onto 24-well plates in DMEM supplemented with 10% FBS. After 24 hr, cells were treated with IL-1 (10 ng/ml) (R&D Systems) for 16 hr. The concentration of IL-6 in the culture supernatants was determined by ELISA (R&D Systems).

Northern blot analysis

Total RNA was prepared from MEFs using Trizol (GIBCO BRL). RNA (20 μg) was fractionated on a 1% formaldehyde gel and transferred onto a Hybond N membrane (Amersham). Filters were hybridized at 65°C in 50% formamide, 5× SSC, 25 mM Na_2HPO_4 (pH 6.5), 8× Denhardt's solution, 0.5 mg/ml salmon sperm DNA, and 1% SDS with a random priming probe corresponding to the full-length murine *IκBα* cDNA or a *β-actin* cDNA as a control.

MEF cell death assay (PI/AnnexinV-FITC staining)

MEFs (2×10^5) were plated onto six-well plates 24 hr prior to induction with various concentrations of TNFα (R&D Systems) alone or TNFα (10 ng/ml) in combination with various concentrations of cycloheximide (Sigma). Cells were harvested and viability was determined by FACS analysis of PI/AnnexinV-FITC staining using an apoptosis detection kit (R&D Systems) according to the manufacturer's instructions.

Acknowledgments

We thank Alain Israel for providing the *NEMO* antiserum as well as GST–IκBα (1–72) and GST–IκBα (1–72) S/A expression plasmids, Mary Saunders for scientific editing, Malte Peters and Scott Pownall for critically reading the manuscript, Denis Bouchard for technical expertise, and Irene Ng for expert administrative assistance. D.R. was supported by a fellowship of the Deutsche Forschungsgemeinschaft.

The publication costs of this article were defrayed in part by payment of page charges. This article must therefore be hereby marked "advertisement" in accordance with 18 USC section 1734 solely to indicate this fact.

References

Akira, S. and T. Kishimoto. 1992. IL-6 and NF-IL6 in acute-phase response and viral infection. *Immunol. Rev.* **127:** 25–50.

Baeuerle, P.A. and T. Henkel. 1994. Function and activation of *NF-κB* in the immune system. *Annu. Rev. Immunol.* **12:** 141–179.

Beg, A.A. and D. Baltimore. 1996. An essential role for *NF-κB* in preventing TNF-α-induced cell death. *Science* **274:** 782–784.

Beg, A.A., W.C. Sha, R.T. Bronson, S. Ghosh, and D. Baltimore. 1995. Embryonic lethality and liver degeneration in mice lacking the *RelA* component of *NF-κB*. *Nature* **376:** 167–170.

Cohen, L., W.J. Henzel, and P.A. Baeuerle. 1998. *IKAP* is a scaffold protein of the IκB kinase complex. *Nature* **395:** 292–296.

DiDonato, J., F. Mercurio, C. Rosette, J. Wu-Li, H. Suyang, S. Ghosh, and M. Karin. 1996. Mapping of the inducible IκB phosphorylation sites that signal its ubiquitination and degradation. *Mol. Cell. Biol.* **16:** 1295–1304.

DiDonato, J.A., M. Hayakawa, D.M. Rothwarf, E. Zandi, and M. Karin. 1997. A cytokine-responsive IκB kinase that activates the transcription factor *NF-κB*. *Nature* **388:** 548–554.

Doi, T.S., M.W. Marino, T. Takahashi, T. Yoshida, T. Sakakura, L.J. Old, and Y. Obata. 1999. Absence of tumor necrosis factor rescues *RelA*-deficient mice from embryonic lethality. *Proc. Natl. Acad. Sci.* **96:** 2994–2999.

Hu, Y., V. Baud, M. Delhase, P. Zhang, T. Deerinck, M. Ellisman, R. Johnson, and M. Karin. 1999. Abnormal morphogenesis but intact IKK activation in mice lacking the *IKKα* subunit of IκB kinase. *Science* **284:** 316–320.

Jin, D.Y. and K.T. Jeang. 1999. Isolation of full-length cDNA and chromosomal localization of human *NF-κB* modulator *NEMO* to Xq28. *J. Biomed. Sci.* **6:** 115–120.

Li, Q., Q. Lu, J.Y. Hwang, D. Buscher, K.F. Lee, J.C. Izpisua-Belmonte, and I.M. Verma. 1999a. *IKK1*-deficient mice exhibit abnormal development of skin and skeleton. *Genes & Dev.* **13:** 1322–1328.

Li, Q., D. Van Antwerp, F. Mercurio, K.F. Lee, and I.M. Verma. 1999b. Severe liver degeneration in mice lacking the *IκB kinase 2* gene. *Science* **284:** 321–325.

Li, Z.W., W. Chu, Y. Hu, M. Delhase, T. Deerinck, M. Ellisman, R. Johnson, and M. Karin. 1999. The *IKKβ* subunit of *IκB* kinase (IKK) is essential for *NF-κB* activation and prevention of apoptosis. *J. Exp. Med.* **189:** 1839–1845.

Mercurio, F., H. Zhu, B.W. Murray, A. Shevchenko, B.L. Bennett, J. Li, D.B. Young, M. Barbosa, M. Mann, A. Manning et al. 1997. *IKK-1* and *IKK-2*: Cytokine-activated *IκB* kinases essential for *NF-κB* activation. *Science* **278:** 860–866.

Mercurio, F., B.W. Murray, A. Shevchenko, B.L. Bennett, D.B. Young, J.W. Li, G. Pascual, A. Motiwala, H. Zhu, M. Mann et al. 1999. *IκB kinase* (*IKK*)*-associated protein 1*, a common component of the heterogeneous IKK complex. *Mol. Cell. Biol.* **19:** 1526–1538.

Regnier, C.H., H.Y. Song, X. Gao, D.V. Goeddel, Z. Cao, and M. Rothe. 1997. Identification and characterization of an *IκB* kinase. *Cell* **90:** 373–383.

Rothwarf, D.M., E. Zandi, G. Natoli, and M. Karin. 1998. *IKKγ* is an essential regulatory subunit of the IkappaB kinase complex. *Nature* **395:** 297–300.

Scott, M.L., T. Fujita, H.C. Liou, G.P. Nolan, and D. Baltimore. 1993. The p65 subunit of *NF-κB* regulates IκB by two distinct mechanisms. *Genes & Dev.* **7:** 1266–1276.

Takeda, K., O. Takeuchi, T. Tsujimura, S. Itami, O. Adachi, T. Kawai, H. Sanjo, K. Yoshikawa, N. Terada, and S. Akira. 1999. Limb and skin abnormalities in mice lacking *IKKα*. *Science* **284:** 313–316.

Tanaka, M., M.E. Fuentes, K. Yamaguchi, M.H. Durnin, S.A. Dalrymple, K.L. Hardy, and D.V. Goeddel. 1999. Embryonic lethality, liver degeneration, and impaired *NF-κB* activation in *IKKβ*-deficient mice. *Immunity* **10:** 421–429.

Van Antwerp, D.J., S.J. Martin, T. Kafri, D.R. Green, and I.M. Verma. 1996. Suppression of TNFα-induced apoptosis by *NF-κB*. *Science* **274:** 787–789.

Verma, I.M., J.K. Stevenson, E.M. Schwarz, D. Van Antwerp, and S. Miyamoto. 1995. *Rel/NFκB/IκB* family: Intimate tales of association and dissociation. *Genes & Dev.* **9:** 2723–

2735.
Wang, C.Y., M.W. Mayo, and A.S. Baldwin, Jr. 1996. TNF- and cancer therapy-induced apoptosis: Potentiation by inhibition of *NF-κB*. *Science* **274:** 784–787.
Woronicz, J.D., X. Gao, Z. Cao, M. Rothe, and D.V. Goeddel. 1997. *IκB kinase-β: NF-κB* activation and complex formation with *IκB kinase-α* and *NIK*. *Science* **278:** 866–869.
Yamaoka, S., G. Courtois, C. Bessia, S.T. Whiteside, R. Weil, F. Agou, H.E. Kirk, R.J. Kay, and A. Israel. 1998. Complementation cloning of *NEMO*, a component of the IκB kinase complex essential for *NF-κB* activation. *Cell* **93:** 1231–1240.
Yeh, W.C., A. Shahinian, D. Speiser, J. Kraunus, F. Billia, A. Wakeham, J.L. de la Pompa, D. Ferrick, B. Hum, N. Iscove et al. 1997. Early lethality, functional *NF-κB* activation, and increased sensitivity to TNF-induced cell death in *TRAF2*-deficient mice. *Immunity* **7:** 715–725.
Zandi, E., D.M. Rothwarf, M. Delhase, M. Hayakawa, and M. Karin. 1997. The IkappaB kinase complex (IKK) contains two kinase subunits, *IKKα* and *IKKβ*, necessary for IκB phosphorylation and *NF-κB* activation. *Cell* **91:** 243–252.